

A Backstepping-Like Coordinated Excitation and SVC Controller Design of Power Systems

A. KANCHANAHARUTHAI¹, E. MUJJALINVIMUT²

¹Department of Electrical Engineering, Rangsit University
Patumthani 12000, Thailand, Email: adirak@rsu.ac.th

²Department of Electrical Engineering, King Mongkut's University of Technology Thonburi
Bangkok, THAILAND Email: ekkachai.muj@kmutt.ac.th

Abstract: This paper focuses on the design of a backstepping-like nonlinear coordinated controller for excitation and static var compensator (SVC) of an electrical power system to enhance transient stability and voltage regulation after the occurrence of a large disturbance and a small perturbation. Based on this scheme, the developed nonlinear controller is used to not only achieve power angle stability, frequency and voltage regulation but also ensure that the closed-loop system is transiently and asymptotically stable. Besides, the developed design technique is rather simple but effective as compared with an immersion and invariance (I&I) control technique and a traditional backstepping nonlinear design technique. In order to show the effectiveness of the proposed controller design, the simulation results illustrate that in spite of the case where a large perturbation occurs on the transmission line or there is a small perturbation to mechanical power inputs, the proposed controller can not only keep the system transiently stable but also simultaneously accomplish good dynamic properties of the system as compared to operation with the existing nonlinear controllers.

Key-Words: Transient stability, backstepping-like nonlinear controller, generator excitation, SVC

1 Introduction

On account of the rapid increase of the size and complexity of power systems, power system stability, including power angle stability as well as frequency and voltage regulation, is of great importance. In general, the stability margins of the power system decrease as the electrical power transmission levels increase. It is well-known that recently the power system operation is faced with the difficult task of maintaining stability when small or large disturbances occur in the power system. Therefore, more effective and efficient control methodologies for improvement of power system stability are desired. In particular, to enhance power system stability margins and accomplish transfer limits, an advanced nonlinear controller design has attracted much attention in literature for years.

Although there have been numerous studies for power system stability enhancement, recently an effective approach to improving the stability of power systems uses generator excitation control in combination with flexible ac transmission systems (FACTS) devices. FACTS devices [1]-[15] are becoming increasingly important for the controllability improvement of power flows and voltages as well as the stability of the power systems. FACTS devices include SVC, static synchronous compensator (STATCOM), thyristor-controlled series compensator (TCSC), static

series synchronous compensator (SSSC), thyristor-controlled phase angle regulator (TCPAR), unified power flow controller (UPFC), etc., and these devices are often employed in interconnected and long-distance transmission systems to improve power flow, voltage control, inter-area and system oscillations, reactive power control, steady-state and dynamic stability. In this paper, among a family of these FACTS devices, of particular interest is the Static Var Compensator (SVC) because it is the most popular type of FACTS devices [4, 5]. This device can regulate the system voltage and improve power system stability. In particular it is able to provide fast-acting reactive power to increase grid transfer capability through enhanced dynamic voltage stability, provides smooth and rapid reactive power compensation for voltage support, and improves both damping oscillations and transient stability [4]-[9]. In [4]-[6], the SVC damping controller design was proposed via optimization algorithms to enhance power system stability. In [7]-[9], with the help of robust control techniques, a coordinated generator excitation and SVC controller was presented for transient stability improvement and voltage regulation.

Unfortunately, there was an important disadvantage in using those controllers. That is, the operating condition can change at any time while the desired lin-

ear and robust controllers designed around the original steady-state operating point. This causes insufficient robustness of the power system since the designed controller performance cannot be guaranteed under the widely changing operating condition. A natural way to address such problems is to adopt a stabilizing feedback control for nonlinear power systems using nonlinear control theory.

Lately, although considerable research above has been paid to the application of SVC mentioned previously, less attention has been devoted to the coordination of generator excitation and SVC controller for power systems via directly the nonlinear control theory. The exact linearization feedback control of SVC system was investigated in [10]. With the help of the feedback linearization method and control of differential and algebraic systems, a coordinated generator excitation and SVC controller in power systems with nonlinear loads was proposed and it can improve the power angle stability of generators and the voltage behavior [11]. A nonlinear controller design for SVC to improve power system voltage stability using direct feedback linearization technique was studied in [12]. Based on adaptive and robust control technique, the SVC controller was capable of enhancing power system voltage stability [13]. More recently, in [14], based on modifying adaptive backstepping sliding model control methodology an adaptive backstepping sliding mode \mathcal{H}_∞ controller was proposed for static var compensator alone. The controller not only attenuates the influences of external disturbances on the system output, but also has strong robustness for system parameter variations. Recently, in [15], an immersion and invariance (I&I) design technique was proposed for the design of a nonlinear coordinated generator excitation and SVC controller for transient stability enhancement and voltage regulation of power systems.

This paper continues this line of investigation but determine a simpler nonlinear controller design procedure than the one from our previous work reported in [15]. From our previous work, the resulting nonlinear I&I controller highly relies upon selecting a target dynamical system capturing the desired behavior of the closed-loop system to be controlled. Besides, the aim of the obtained control law is to ensure that the closed-loop system behaves asymptotically the same as the pre-specified target system. Even though the I&I control methodology is most effective and applicable to practical control design problems for various types of systems [16]-[21], there are significant difficulties once used to design the desired nonlinear controller. This makes the design procedure rather further complicated. Therefore, this paper proposes a nonlinear controller via a backstepping-like procedure as

reported in [22] in order to overcome many difficulties. The proposed controller is not only considerably simple, but also effective in comparison with the I&I one. Based on this simple scheme, the developed controller is designed to not only simultaneously achieve power angle stability along with frequency and voltage regulation, but also keep the closed-loop system transiently stable similar to the I&I one.

The paper is organized as follows. Section 2 presents the dynamic models of the synchronous generator and SVC and the control problem definition. Section 3 present the backstepping-like controller design. Then, Simulation results are given in Section 4. We conclude in Section 5. Finally, Appendix follows thereafter.

2 Power System Models with SVC

The dynamic models of power systems consist of the dynamics of a synchronous generator and SVC. A dynamic model of the synchronous generator (SG) can be obtained by representing the SG by a transient voltage source, E , behind a transient reactance, X'_d . In this paper, as shown in Figure 1, a thyristor-controlled-reactor (TCR) fixed-capacitor type of SVC is used and the SVC can serve as a variable susceptance connected in shunt the power system [14]. For simplicity, the dynamic model of the SVC is often modeled as a first-order differential equation. Consequently, the dynamics of synchronous generator with excitation control and the SVC regulator in SMIB power systems can be modeled as follows [12]:

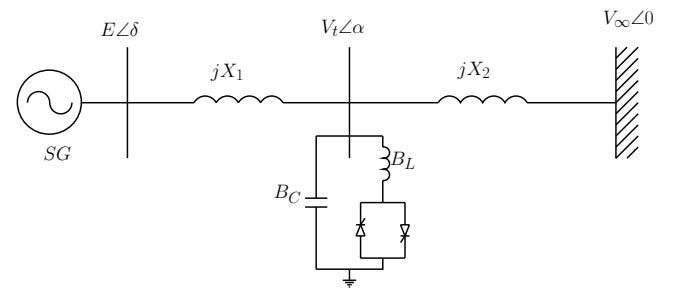


Figure 1: Network with TCR-FC SVC [15]

$$\begin{cases} \dot{\delta} &= \omega - \omega_s, \\ \dot{\omega} &= \frac{1}{M} (P_m - P_E - D(\omega - \omega_s)), \\ \dot{E} &= -\frac{X_{d\Sigma}}{X'_d T_0} E + \frac{X_d - X'_d}{X'_d T_0} V_\infty \cos \delta + \frac{u_f}{T_0}, \\ \dot{B}_L &= \frac{1}{T_r} (B_L - B_{L0} + u_r), \end{cases} \quad (1)$$

with

$$P_E = \frac{EV_\infty \sin \delta}{X'_{d\Sigma} - (X'_d + X_T)X_L(B_L - B_C)},$$

where δ is the power angle of the generator, ω denotes the relative speed of the generator, $D \geq 0$ is a damping constant, P_E is the electrical power delivered by the generator to the voltage at the infinite bus V_∞ , ω_s is the synchronous machine speed, $\omega_s = 2\pi f$, H represents the per unit inertial constant, f is the system frequency and $M = 2H/\omega_s$, $X'_{d\Sigma} = X'_d + X_T + X_L$ is the reactance consisting of the direct axis transient reactance of SG, the reactance of the transformer, and the reactance of the transmission line X_L . Similarly, $X_{d\Sigma} = X_d + X_T + X_L$ is identical to $X'_{d\Sigma}$ except that X_d denotes the direct axis reactance of SG. T'_0 is the d-axis transient short-circuit time constant. $X_1 = X'_d + X_T$, $X_2 = X_L$, u_f is the field voltage control input. P_m is the mechanical input power to be assumed constant throughout this paper. B_L and B_C are the susceptance of the inductor in SVC (pu) and the equivalent capacitor (pu.), B_{L0} is the initial value of the inductor in SVC (pu.), u_r is the SVC control input to be designed, and T_r is a SVC time constant.

Practically, the generator transient voltage (E) is often physically unmeasurable and $B_L - B_C$ may not be convenient to monitor like active electrical power, thus the active power P_E can be divided into two new variables, namely, an active electrical power of generation excitation alone P_e and a real electrical power of the SVC device P_{svc} below:

$$\begin{cases} P_E &= P_e + P_{svc}, \\ P_e &= \frac{EV_\infty \sin \delta}{X'_{d\Sigma}}, \\ P_{svc} &= \frac{(X'_d + X_T)X_L(B_L - B_C)}{X'_{d\Sigma} - (X'_d + X_T)X_L(B_L - B_C)} \frac{EV_\infty \sin \delta}{X'_{d\Sigma}}, \\ &= \frac{(X'_d + X_T)X_L(B_L - B_C)}{X'_{d\Sigma} - (X'_d + X_T)X_L(B_L - B_C)} P_e. \end{cases} \quad (2)$$

Remark 1 In this paper the SMIB power system with SVC as shown in Figure 1 is considered. However, we can extend the proposed strategy to multi-machine systems. This makes the developed design procedure further complicated and will be presented in the future.

After defining the state variables $x = [x_1, x_2, x_3, x_4]^T = [\delta - \delta_e, \omega - \omega_s, P_e, P_{svc}]^T$, we have the dynamic model of power systems with SVC that can be expressed as (3)-(4).

Further, the bus (terminal) voltage V_t as shown in Figure 1 can be found from the following expression

$$\begin{aligned} V_t &= \left(1 + \frac{x_4}{x_3}\right) \cdot \frac{\Delta(x_1, x_3)}{X'_{d\Sigma}} \\ \Delta(x_1, x_3) &= \left[\left(\frac{x_3 X'_{d\Sigma} X_2}{V_\infty \sin(x_1 + \delta_e)} \right)^2 + (V_\infty X_1)^2 \right. \\ &\quad \left. + 2X_1 X_2 X'_{d\Sigma} x_3 \cot(x_1 + \delta_e) \right]^{1/2} \end{aligned}$$

Additionally, the region of operation is defined in the set $\mathcal{D} = \{x \in \mathcal{S} \times \mathbb{R} \times \mathbb{R} \times \mathbb{R} \mid 0 < x_1 < \frac{\pi}{2}\}$. The open loop operating equilibrium is denoted by $x_e = [x_{1e}, x_{2e}, x_{3e}, x_{4e}]^T = [0, 0, P_m, 0]^T$. From the dynamic equations (3) above, it is easy to see that all state variables (x_1, x_2, x_3, x_4) are measurable and such state variables can be used to find the bus voltage V_t .

Therefore, the objective of this paper is to design a state feedback control law that meets the following expected performance requirements:

1. the equilibrium point x_e is asymptotically stable,
2. power angle stability along with voltage and frequency regulation are simultaneously achieved.

Consider the model stated above, it is easy to see that all state variables can be measured in this system. In (3)-(4), there is also a nonlinear controller $u = [u_f/T'_0, u_r/T_r]^T$ to be designed. For notational convenience, the nonlinear power system¹ in (3)-(4) can be rewritten as follows.

$$\begin{cases} \dot{x}_1 &= x_2 \\ \dot{x}_2 &= \frac{1}{M}(P_m - Dx_2 - x_3 - x_4) \\ \dot{x}_3 &= f_3(x) + g_{31}(x) \frac{u_f}{T'_0} \\ \dot{x}_4 &= f_4(x) + g_{41}(x) \frac{u_f}{T'_0} + g_{42}(x) \frac{u_r}{T_r} \end{cases} \quad (6)$$

Thus, the objective of this paper is to solve the problem of the transient stabilization of the system (6) to design a coordinated stabilizing (state) feedback controller u such that the resulting closed-loop system is asymptotically stable at the only equilibrium (x_e) and $x \rightarrow x_e$ as $t \rightarrow \infty$.

Remark 2 It is obvious that the dynamics of x_2 rely on the state variables x_3 and x_4 . Therefore, the dynamic equations (6) is not of the strict-feedback form [23] for backstepping design. However, backstepping design, compared with the proposed design in this paper, needs to be further extended for the design of nonlinear controllers, see Appendix.

3 Backstepping-Like Controller Design

For the purpose of designing a nonlinear controller such that $\lim_{t \rightarrow +\infty} x_i = 0$, ($i = 1, 2, 4$), $\lim_{t \rightarrow +\infty} x_3 = P_m$, let us take the following Lyapunov candidate as follows:

$$V_1 = \frac{1}{2} x_1^2 \quad (7)$$

¹It is assumed that all functions are C^∞ throughout this paper.

$$\dot{x} = f(x) + g(x)u(x) \tag{3}$$

with

$$\left\{ \begin{aligned} f(x) &= \begin{bmatrix} f_1(x) \\ f_2(x) \\ f_3(x) \\ f_4(x) \end{bmatrix} = \begin{bmatrix} x_2 \\ \frac{1}{M} (P_m - Dx_2 - x_3 - x_4) \\ (-a + x_2 \cot(x_1 + \delta_e))x_3 + \frac{bV_\infty \sin 2(x_1 + \delta_e)}{X'_{d\Sigma}} \\ \tilde{M}(x_1, x_3, x_4)f_3(x) + \tilde{N}(x_1, x_3, x_4)(B_L - B_{L0}) \end{bmatrix}, \\ g(x) &= \begin{bmatrix} 0 & 0 \\ 0 & 0 \\ g_{31}(x) & 0 \\ g_{41}(x) & g_{42}(x) \end{bmatrix} = \begin{bmatrix} 0 & 0 \\ 0 & 0 \\ \frac{V_\infty \sin(x_1 + \delta_e)}{X'_{d\Sigma}} & 0 \\ \tilde{M}(x_1, x_3, x_4)g_{31}(x) & -\tilde{N}(x_1, x_3, x_4) \end{bmatrix}, u(x) = \begin{bmatrix} \frac{u_f}{T'_0} \\ \frac{u_r}{T_r} \end{bmatrix} \end{aligned} \right. \tag{4}$$

where

$$\left\{ \begin{aligned} \tilde{M}(x_1, x_3, x_4) &= \left(\frac{X'_{d\Sigma}}{X'_{d\Sigma} - (X'_d + X_T)X_L(B_L - B_C)} - 1 \right), B_L = \frac{1}{(X'_d + X_T)X_L} \left(X'_{d\Sigma} - \frac{x_3 X'_{d\Sigma}}{x_3 + x_4} \right) + B_C, \\ \tilde{N}(x_1, x_3, x_4) &= -\frac{x_3(X'_d + X_T)X_L X'_{d\Sigma}}{(X'_{d\Sigma} - (X'_d + X_T)X_L(B_L - B_C))^2}, a = \frac{X_{d\Sigma}}{X'_{d\Sigma} T'_0}, b = \frac{X_{d\Sigma} - X'_{d\Sigma}}{X'_{d\Sigma} T'_0} V_\infty. \end{aligned} \right. \tag{5}$$

Then the derivative of (7) becomes

$$\dot{V}_1 = x_1 x_2 = -c_1 x_1^2 + x_1(c_1 x_1 + x_2) \tag{8}$$

where $c_1 > 0$. From (8), it is easy to see that the term $x_1(c_1 x_1 + x_2)$ is not always negative; thus, this term should be eliminated from the aforementioned equation. In order to do this, we choose the Lyapunov function candidate as:

$$V_2 = \frac{1}{2}x_1^2 + \frac{1}{2}(c_1 x_1 + x_2)^2 \tag{9}$$

After calculating the derivative of (9), we have

$$\begin{aligned} \dot{V}_2 &= -c_1 x_1^2 + x_1(c_1 x_1 + x_2) \\ &\quad + (c_1 x_1 + x_2)(c_1 \dot{x}_1 + \dot{x}_2) \\ &= -c_1 x_1^2 + (c_1 x_1 + x_2)(x_1 + c_1 x_2 + \dot{x}_2) \\ &= -c_1 x_1^2 - (c_1 x_1 + x_2)^2 + (c_1 x_1 + x_2) \\ &\quad \times \left[(c + 1)(x_1 + x_2) + \dot{x}_2 \right] \end{aligned} \tag{10}$$

It can be observed that the last term of (10) is not always negative; thus, we should cancel this term.

To this end, we introduce the following terms into V_3 and then obtain

$$V_3 = \frac{1}{2}x_1^2 + \frac{1}{2}(c_1 x_1 + x_2)^2 + \frac{1}{2}\mathcal{P}^2 + \frac{1}{2}\mathcal{Q}^2 \tag{11}$$

where

$$\left\{ \begin{aligned} \mathcal{P} &= (c_1 + 1)\frac{x_1}{2} + (c_1 + 1 - \frac{D}{M})\frac{x_2}{2} + \frac{(P_m - x_3)}{M}, \\ \mathcal{Q} &= (c_1 + 1)\frac{x_1}{2} + (c_1 + 1 - \frac{D}{M})\frac{x_2}{2} - \frac{x_4}{M}. \end{aligned} \right. \tag{12}$$

By calculating the derivative of (11) along the system trajectory, one obtains

$$\begin{aligned} \dot{V}_3 &= -c_1 x_1^2 - (c_1 x_1 + x_2)^2 + \mathcal{P}\dot{\mathcal{P}} + \mathcal{Q}\dot{\mathcal{Q}} \\ &\quad - c_1 x_1^2 - (c_1 x_1 + x_2)^2 \\ &\quad + \mathcal{P} \left[c_1 x_1 + x_2 + (c_1 + 1)\frac{x_2}{3} \right. \\ &\quad \quad \left. + \left(c_1 + 1 - \frac{D}{M} \right) \frac{\dot{x}_2}{2} - \frac{\dot{x}_3}{M} \right] \\ &\quad + \mathcal{Q} \left[c_1 x_1 + x_2 + (c_1 + 1)\frac{x_2}{3} \right. \\ &\quad \quad \left. + \left(c_1 + 1 - \frac{D}{M} \right) \frac{\dot{x}_2}{2} - \frac{\dot{x}_4}{M} \right] \\ &= -c_1 x_1^2 - (c_1 x_1 + x_2)^2 - c_2 \mathcal{P}^2 - c_3 \mathcal{Q}^2 \\ &\quad + \mathcal{P} \left[\tilde{\mathcal{P}} - \frac{\dot{x}_3}{M} \right] + \mathcal{Q} \left[\tilde{\mathcal{Q}} - \frac{\dot{x}_4}{M} \right] \end{aligned} \tag{13}$$

with

$$\left\{ \begin{aligned} \tilde{\mathcal{P}} &= c_2 \mathcal{P} + c_1 x_1 + (c_1 + 3)\frac{x_2}{2} + \left(c_1 + 1 - \frac{D}{M} \right) \frac{\dot{x}_2}{2} \\ \tilde{\mathcal{Q}} &= c_3 \mathcal{Q} + c_1 x_1 + (c_1 + 3)\frac{x_2}{2} + \left(c_1 + 1 - \frac{D}{M} \right) \frac{\dot{x}_2}{2} \end{aligned} \right. \tag{14}$$

where $c_i > 0$, ($i = 1, 2, 3$) are positive design parameters.

After substituting \dot{x}_3 and \dot{x}_4 into (13), one has

$$\begin{aligned} \dot{V}_3 = & -c_1 x_1^2 - (c_1 x_1 + x_2)^2 - c_2 \mathcal{P}^2 - c_3 \mathcal{Q}^2 \\ & + \mathcal{P} \left[\tilde{\mathcal{P}} - \frac{1}{M} \left(f_3(x) + g_{31}(x) \frac{u_f}{T_0} \right) \right] \\ & + \mathcal{Q} \left[\tilde{\mathcal{Q}} - \frac{1}{M} \left(f_4(x) + g_{41}(x) \frac{u_f}{T_0} \right. \right. \\ & \left. \left. + g_{42}(x) \frac{u_r}{T_r} \right) \right] \end{aligned} \quad (15)$$

Therefore, if we choose

$$\begin{cases} \frac{u_f}{T_0} = \frac{1}{g_{31}(x)} \left[-f_3(x) + M\tilde{\mathcal{P}} \right] \\ \frac{u_r}{T_r} = \frac{1}{g_{42}(x)} \left[-f_4(x) - g_{41}(x) \frac{u_f}{T_0} + M\tilde{\mathcal{Q}} \right] \end{cases} \quad (16)$$

Then, under the feedback control law (16), the equation (15) turns into

$$\dot{V}_3 = -c_1 x_1^2 - (c_1 x_1 + x_2)^2 - c_2 \mathcal{P}^2 - c_3 \mathcal{Q}^2 \leq 0 \quad (17)$$

With the help of Lyapunov stability theory, it is obvious that

$$\begin{cases} \lim_{t \rightarrow +\infty} x_1 = 0 \\ \lim_{t \rightarrow +\infty} (c_1 x_1 + x_2) = 0 \\ \lim_{t \rightarrow +\infty} \mathcal{P} = 0 \\ \lim_{t \rightarrow +\infty} \mathcal{Q} = 0 \end{cases} \quad (18)$$

These also imply that $\lim_{t \rightarrow +\infty} x_1 = \lim_{t \rightarrow +\infty} x_2 = \lim_{t \rightarrow +\infty} x_4 = 0$, and $\lim_{t \rightarrow +\infty} x_3 = P_m$. According to the aforementioned discussion, the following theorem obvious holds.

Theorem 3 Consider the nonlinear power system with SVC in (6). Provided that the nonlinear controller is designed by (16), then the equilibrium point of the system (3) is asymptotically stable. This implies that $\lim_{t \rightarrow +\infty} x_i = 0$, ($i = 1, 2, 4$), $\lim_{t \rightarrow +\infty} x_3 = P_m$.

Proof: The proof of Theorem 3 is based on the argument given above.

4 Simulation Results

In this section, in order to demonstrate the application of the proposed scheme, the simulation results of the

coordination between generator excitation and SVC control in a SMIB power system are shown in Figure 1. Power angle stability as well as voltage and frequency regulations is used to point out the transient stability enhancement and dynamic properties.

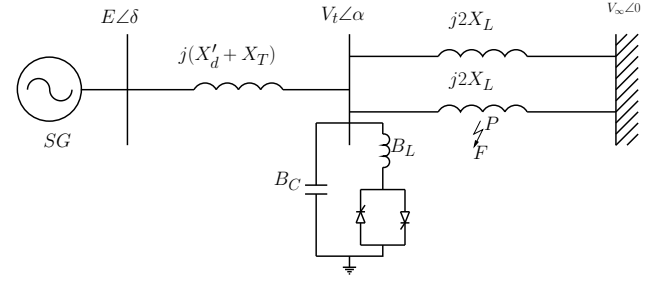


Figure 2: A single line diagram of SMIB with TCR-FC SVC [15]

Considering the single line diagram as shown in Figure 2 where SG is connected through parallel transmission line to an infinite-bus, such SG delivers 1.0 per unit (pu.) power while the terminal voltage V_t is 0.9897 pu, and an infinite-bus voltage is 1.0 pu.

We assume that once there is a three-phase fault (a large perturbation) occurring at the point, the midpoint of one of the transmission lines, leading to rotor acceleration, voltage sag, and large transient induced electromechanical oscillations. Further, assuming that a small perturbation in the mechanical input power occurs on the network, resulting in the system trajectories, induced by the perturbation, confined to a limited region in a neighborhood of a nominal operating trajectory. We are, therefore, interested in the following two questions. One is whether, after the fault is cleared from the network, the system will return to a post-fault equilibrium state or not. The other becomes whether, after the small perturbation disappears, the system can maintain stability or not. In the simulations, the fault of interest is a symmetrical three phase short circuit occurring on one of the transmission lines as shown in Figure 2. The following two cases with a temporary fault sequence and a small perturbation to mechanical power to synchronous generators in the system are discussed.

The physical parameters (pu.) and initial conditions (δ_e , ω_s , P_{ee} , P_{svce}) for this power system model are given as follows:

$$\begin{aligned} \omega_s &= 2\pi f \text{ rad/s}, D = 0.2, H = 5, \\ f &= 60 \text{ Hz}, T_0' = 4, T_r = 0.2; V_\infty = 1 \angle 0^\circ, \\ \omega &= \omega_s, X_d = 1.1, X_d' = 0.2, X_T = 0.1, \\ X_L &= 0.2, T_r = 0.02, \delta_e = 0.4964 \text{ rad}, \\ P_{ee} &= P_m = 1.0 \text{ pu.}, B_{L0} = B_C = 0.3 \end{aligned}$$

The tuning parameters of the control law are set

as $c_1 = c_2 = c_3 = 10$. In this paper, two cases with different fault sequences are investigated in the transient stability studies.

Case 1: Temporary fault

The system is in a pre-fault steady state, a fault occurs at $t_0 = 0.5$ sec., the fault is isolated by opening the breaker of the faulted line at $t_c = 1$ sec., the transmission line is recovered without the fault at $t_r = 1.5$ sec. Afterward the system is in a post-fault state.

Case 2: The mechanical input power increase

The system is in the pre-fault state, at $t = 0.5$ sec., there is a 20% perturbation in the mechanical power ($\Delta P_m(t) = 0.2P_m$ pu.) After $t = 2.5$ sec. the perturbation disappears, then the system is eventually in a post-fault state.

The effectiveness of the proposed strategy is shown by transient stability enhancement of the coordinated (generator excitation/SVC) nonlinear control scheme. Power angle stability, voltage, frequency, and power regulations, are investigated and compared with existing nonlinear controllers, e.g., the I&I controller [15] and the backstepping controller [23] given in Appendix.

For Case 1, it can be seen that Figure 3 shows the time responses of power angle (δ), frequency ($\omega - \omega_s$), transient internal voltage (E), and susceptance of SVC (B_L). These responses return to the pre-fault state values, under the I&I control, the backstepping controller, and the proposed control, respectively. Apart from this, time responses of active power (P_E) and SVC terminal voltage (V_t) are shown in Figure 4. It is obvious that even if the developed design procedure hardly becomes complicated, the proposed controller and the I&I controller provide a similarly good transient behavior over the backstepping scheme. In comparison with the backstepping method, the convergence and damping of the proposed controller are greatly better. In particular, the proposed control provides better transient response performance in terms of reduced overshoot and faster reduction of oscillations.

Similar to Case 1, it is evident from Case 2 that Figures 5-6 illustrate time trajectories of power angle, frequency, transient internal voltage, susceptance of SVC, active power and terminal voltage, respectively. All time trajectories settle to the pre-fault steady state in spite of having a small perturbation of mechanical input power. For this case, the mechanical power is varied from the normal value to some constant (in simulation $P_m = 1$ pu., $\Delta P_m = 0.2$ pu.). It is clear that the equilibrium can be recovered and the terminal voltage can be regulated to the prescribed value when the system is forced by the proposed control. Further, as compared with the backstepping scheme, the proposed controller not only effectively damps the os-

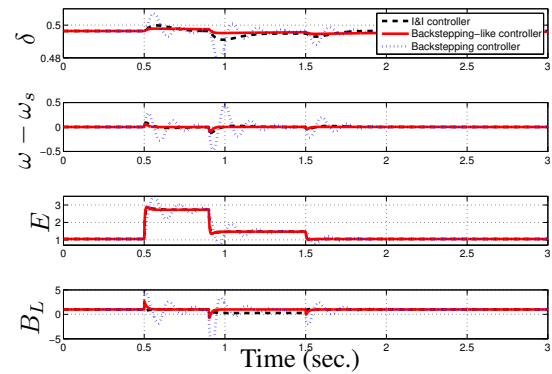


Figure 3: Controller performance in Case 1– Time histories of power angle (δ), relative speed ($\omega - \omega_s$), Transient voltage (E), and Susceptance of SVC (B_L) (Solid: Backstepping-like controller, Dashed: I&I Dotted: Backstepping controller)

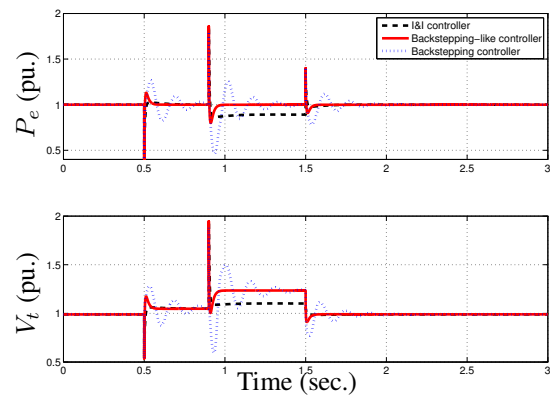


Figure 4: Controller performance in Case 1– Time histories of active power (P_e) and terminal voltage (V_t) (Solid: Backstepping-like controller, Dashed: I&I controller, Dotted: Backstepping controller)

cillations of power angle, frequency, active power and terminal voltage, but also has superior performance in maintaining the terminal bus voltage magnitudes close to their reference voltage values defined for the normal operating conditions. It also provides effective voltage regulation to the desired pre-fault steady-state values after the occurrence of a small perturbation in mechanical power. Besides, time histories of the proposed controller are almost identical to those of the I&I one which is an advance control design technique. On the other hand, the proposed design procedure is very easy as compared with the I&I one. Further it provides better dynamic performance (improved transient responses for the closed-loop system) and is capable of achieving the expected performance require-

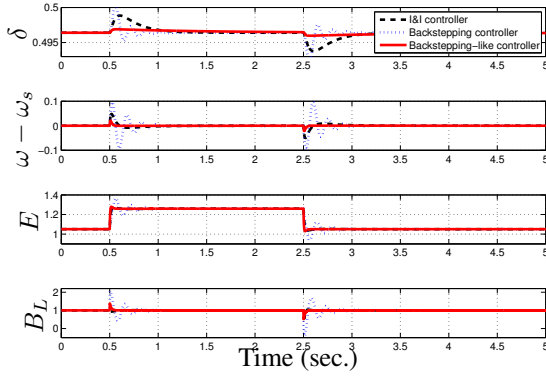


Figure 5: Controller performance in Case 2– Time histories of power angle (δ), relative speed ($\omega - \omega_s$), Transient voltage (E), and Susceptance of SVC (B_L) (Solid: Backstepping-like controller, Dashed: I&I controller, Dotted: Backstepping controller)

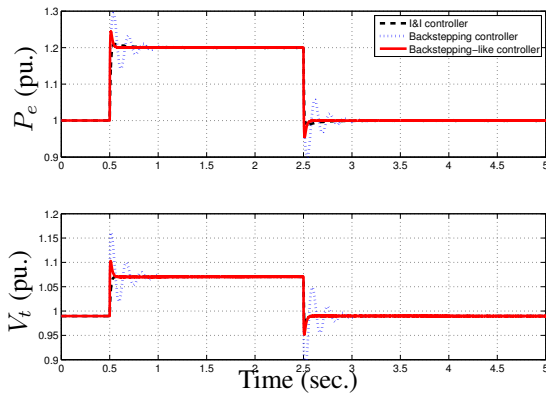


Figure 6: Controller performance in Case 2– Time histories of active power (P_e) and terminal voltage (V_t) (Solid: Backstepping-like controller, Dashed: I&I controller, Dotted: Backstepping controller)

ments 1)-2) mentioned above. .

As indicated in the simulation results above. It can be, overall, concluded that the proposed control law is effectively designed for transient stabilization and voltage regulation following short circuit and mechanical input change conditions. Similar to the advanced (I&I) controller, the proposed control law can render the closed-loop system converge quickly to a equilibrium point; meanwhile the active power and the terminal voltage can be quickly regulated to the reference values. Even though the developed design procedure becomes considerably simple, the time responses of the proposed scheme do slightly differ from those of the I&I one. Also the proposed strategy obviously outperforms the backstepping one in terms of fast con-

vergence speed and smaller overshoot magnitude.

5 Conclusion

In this paper, a backstepping-like nonlinear controller for a single-machine infinite-bus power system with a nonlinear generator excitation and SVC has been proposed to improve effectively the transient stability, power angle stability as well as frequency and voltage regulations. In contrast with the previous work [15] having the complicated design procedure, in this paper the proposed controller is rather simpler. Additionally, the current simulation results have demonstrated that despite the simple design procedure, power angle stability along with voltage and frequency regulations are achieved following the large (transient) disturbances on the network via nonlinear model-based backstepping-like control design technique. In particular, in spite of the occurrence of severe disturbances on the transmission line and a small perturbation of mechanical input power, the closed-loop system will be driven to a stable equilibrium under the proposed control method. The performance of the proposed control is compared with that of the I&I one and the backstepping one, respectively. It can be observed that the damping and the closed-loop system dynamics of the proposed control do not differ much from those of the I&I one but perform much better than those of the backstepping one. In addition, the presented controller simultaneously achieves transient stabilization and accomplishes a good regulation of the SVC terminal voltage. As future works, it is interesting to consider the extension of this strategy to robust control design in the presence of disturbance and unknown parameters of power systems.

6 Appendix

Backstepping Controller Design [23]

In order to design a nonlinear adaptive controller based on backstepping scheme used to compare with the proposed adaptive controller, let us define the state variable by $x_1 = \delta - \delta_e, x_2 = \omega - \omega_s, x_3 = P_e - P_{ee}, x_4 = P_{svc} - P_{svce}, e_i = x - x_i^*, (i = 1, 2, 3, 4), x_1^* = 0, x_2^* = -c_1 x_1, x_3^* = M e_1 + \frac{c_2 e_2}{2} + P_m - D x_2, x_4^* = c_1 M x_2 + \frac{c_2 e_2}{2}$. Hence, the backstepping control approach is expressed in the following Proposition.

Theorem 4 Consider the system (6), the adaptive

backstepping control law is as follows:

$$\begin{cases} \frac{u_f(x)}{T_0} = \frac{1}{g_{31}(x)} \left[\frac{e_2}{M} - f_3(x) + (M + \frac{c_1 c_2}{2})x_2 \right. \\ \quad \left. + (\frac{c_2}{2} - D)\dot{x}_2 - c_3 e_3 \right] \\ \frac{u_r(x)}{T_r} = \frac{1}{g_{42}(x)} \left[\frac{e_2}{M} - f_4(x) - g_{41}(x) \frac{u_f}{T_0} \right. \\ \quad \left. + (\frac{c_2}{2} + c_1 M) \dot{x}_2 + \frac{c_1 c_2 x_2}{2} - c_4 e_4 \right] \end{cases} \quad (19)$$

where $c_i > 0, (i = 1, 2, 3, 4)$ are positive design parameters. Then, the overall closed-loop system with the controller above is asymptotically stable. In this work, tuning parameters are chosen as $c_1 = c_3 = c_4 = 20, c_2 = 2$.

Proof: In the following, the control law is designed by the backstepping scheme.

Step 1: For the first subsystem of the system (6), x_2 is considered as the virtual control variable. Then, the virtual control of x_2 is designed as $x_2^* = -c_1 x_1$, where $c_1 > 0$ is a design constant. Let us define the error variable $e_2 = x_2 - x_2^*$ and $e_1 = x_1$. Then, we have

$$\dot{e}_1 = e_2 - c_1 e_1 \quad (20)$$

For the system (20), we choose the Lyapunov function as $V_1 = \frac{1}{2}e_1^2$. The time derivative of V_1 along the system trajectory is

$$\dot{V}_1 = e_1(e_2 - c_1 e_1) = -c_1 e_1^2 + e_1 e_2. \quad (21)$$

It is clear that $\dot{V}_1 \leq 0$ where $e_2 = 0$.

Step 2: Let us define the augmented Lyapunov function of Step 1 as $V_2 = V_1 + \frac{1}{2}e_2^2$. Notice that

$$\begin{aligned} \dot{e}_2 &= \dot{x}_2 - \dot{x}_2^* \\ &= \frac{1}{M}(P_m - Dx_2 - x_3 - x_4) + c_1 x_2 \end{aligned} \quad (22)$$

Then the time derivative of V_2 along the system trajectory is

$$\begin{aligned} \dot{V}_2 &= \dot{V}_1 + e_2 \dot{e}_2 = -c_1 e_1^2 \\ &\quad + e_2 \left[e_1 + \frac{1}{M}(P_m - Dx_2 - x_3 - x_4) + c_1 x_2 \right] \end{aligned} \quad (23)$$

From (22), x_3 and x_4 are taken as the virtual control variables. Define the error variables $e_3 = x_3 - x_3^*$ and $e_4 = x_4 - x_4^*$. Then two virtual control variables

are chosen as $x_3^* = Me_1 + P_m - Dx_2 + \frac{c_2 e_2}{2}$ and $x_4^* = c_1 M x_2 + \frac{c_2 e_2}{2}$, respectively. Then it holds

$$\dot{V}_2 = -c_1 e_1^2 - c_2 e_2^2 - \frac{e_2}{M}(e_3 + e_4) \quad (24)$$

Step 3: Let us define the augmented Lyapunov function of Step 2 by

$$V_3 = V_2 + \frac{1}{2}(e_3^2 + e_4^2) \quad (25)$$

In addition, note that $e_i = x_i - x_i^*, (i = 3, 4)$, the time derivative of V_3 along the system trajectory becomes

$$\begin{aligned} \dot{V}_3 &= \dot{V}_2 + e_3 \dot{e}_3 + e_4 \dot{e}_4 \\ &= -c_1 e_1^2 - c_2 e_2^2 \\ &\quad + e_3 \left[-\frac{e_2}{M} + f_3(x) + g_{31}(x) \frac{u_f}{T_0} \right. \\ &\quad \left. - (M + \frac{c_1 c_2}{2})x_2 - (\frac{c_2}{2} - D)\dot{x}_2 \right] \\ &\quad + e_4 \left[-\frac{e_2}{M} + f_4(x) + g_{41}(x) \frac{u_f}{T_0} \right. \\ &\quad \left. + f_{42}(x) \frac{u_r}{T_r} - (\frac{c_2}{2} + c_1 M) \dot{x}_2 - \frac{c_1 c_2 x_2}{2} \right]. \end{aligned} \quad (26)$$

We can choose the feedback control law as given in (19), thereby resulting in $\dot{V}_3 = -\sum_{i=1}^4 c_i e_i^2 \leq 0$, where $c_i > 0, (i = 1, 2, 3, 4)$ are positive constants.

Thus, under the feedback control law (19), the error system representation of the resulting closed-loop adaptive system:

$$\begin{cases} \dot{e}_1 = e_2 - c_1 e_1, \\ \dot{e}_2 = -c_2 e_2 - e_3 - e_4, \\ \dot{e}_3 = -c_3 e_3 \\ \dot{e}_4 = -c_4 e_4 \end{cases} \quad (27)$$

is asymptotically stable. It is easy to see from (26) that $\dot{V}_3 \leq 0$. This implies that based on Lyapunov stability theory, $\lim_{t \rightarrow +\infty} e_i = 0, (i = 1, 2, 3, 4)$ and from the definition, the system state variables x_i and x_i^* also converge to zero as t goes to infinity. This completes the proof.

References:

- [1] N. G. Hingorani and L. Gyugyi, *Understanding FACTS: Concepts and Technology of flexible AC Transmission Systems*, IEEE Press:– New Jersey 1999
- [2] Y. N. Song and A. T. John, *Flexible AC Transmission Systems (FACTS)*, IEE Power and Energy Series 30,–London 1999

- [3] S. M. Abd-Elazim, and E. S. Ali, Synergy of Particle Swarm Optimization and Bacterial Foraging for TCSC Damping Controller Design, *WSEAS Transactions on Power Systems*, 8, 2013, pp. 74-84.
- [4] S. M. Abd-Elazim, and E. S. Ali, Bacteria Foraging Optimization Algorithm Based SVC Damping Controller Design for Power System Stability Enhancement, *International Journal of Electrical Power and Energy Systems*, 43, 2012, pp. 933-940.
- [5] E. S. Ali, S. M. Abd-Elazim, Coordinated Design of PSSs and SVC via Bacteria Foraging Optimization Algorithm in a Multimachine Power System, *International Journal of Electrical Power and Energy Systems*, 41, 2012, pp. 44-53.
- [6] A. Y. Abd-Elaziz, and E. S. Ali, Static VAR Compensator Damping Controller Design Based on Flower Pollination Algorithm for a Multimachine Power System, *Electric Power Components and System*, 43, 2015, pp. 1268-1277.
- [7] K. T. Law, D. J. Hill, and N. R. Godfrey, Robust controller structure for coordinated power system voltage regulator and stabilizer design, *Trans. on Control Systems Technology*, 2, 1994, pp. 220-232.
- [8] T. Cong, Y. Wang, and D. J. Hill, Transient stability and voltage regulation enhancement via coordinated control of generator excitation and SVC, *International Journal of Electrical Power and Energy Systems*, 27, 2005, pp. 121-130.
- [9] T. Cong, Y. Wang, and D. J. Hill, Co-ordinated control design of generator excitation and SVC for transient stability and voltage regulation enhancement of multi-machine power systems, *International Journal of Robust and Nonlinear Control*, 14, 2004, pp. 789-805.
- [10] Q. Lu, Y. Sun, and S. Mei, *Nonlinear Control Systems and Power System Dynamics*, Kluwer Academic Publishers, 2001
- [11] Y. Ruan, and J Wang, The coordinated control of SVC and excitation of generators in power systems with nonlinear loads, *International Journal of Electrical Power and Energy Systems*, 27, 2005, pp. 550-555.
- [12] Y. Wang, H. Chen, and R. Zhou, A nonlinear controller design for SVC to improve power system voltage stability, *International Journal of Electrical Power and Energy Systems*, 22, 2000, pp. 463-470.
- [13] R. Yan, Z. Y. Dong, T. K Saha, and J. Ma, Non-linear robust adaptive SVC controller design for power systems, *Proceedings of Power Energy Soc. General Meet.*, 2008, pp. 1-7.
- [14] L.-Y. Sun, S. Tong, and Y. Liu, Adaptive backstepping sliding mode \mathcal{H}_∞ control of static var compensator, *IEEE Transactions on Control Systems Technology*, 19, 2011, pp. 1178-1185.
- [15] A. Kanchanahanathai, Immersion and invariance-based coordinated generator excitation and SVC control for power systems. *Mathematical Problems in Engineering*, 2014, pp. 1-11.
- [16] A. Astolfi and R. Oreta, Immersion and invariance: a new tool for stabilization and adaptive control of nonlinear systems, *IEEE Transactions on Automatic Control*, 48, 2003, pp. 590-606.
- [17] A. Astolfi, D. Karagiannis, and R. Oreta, *Nonlinear and Adaptive Control Design with Applications*, Springer-Verlag, London 2007
- [18] A. Kanchanahanathai, Immersion and invariance-based nonlinear dual-excitation and steam-valving control of synchronous generators. *International Transactions on Electrical Energy Systems*, 24, 2014, pp. 1671-1687.
- [19] A. Kanchanahanathai, Immersion and invariance-based non-linear coordinated control for generator excitation and static synchronous compensator for power systems, *Electric Power Components and Systems*, 42, 2014, pp. 1004-1015.
- [20] A. Kanchanahanathai, V. Chankong, and K. A. Loparo, K. A. Nonlinear generator excitation and superconducting magnetic energy storage control for transient stability enhancement via immersion and invariance, *Transactions of the Institute of Measurement and Control*, 37, 2015, pp.1217-1231.
- [21] N. S. Manjarekar, and R. N. Banavar, "Nonlinear Control Synthesis for Electrical Power Systems Using Controllable Series Capacitors," Springer-Verlag, London, 2012.
- [22] R. Luo, The robust adaptive control of chaotic systems with unknown parameters and external disturbance via a scalar input. *International Journal of Adaptive Control and Signal Processing*, 29, 2015, pp. 1296-1307.
- [23] M. Krstic, I. Kanellakopoulos, and P. Kokotovic, *Nonlinear and Adaptive Control Design*, John Willey & Sons, New York 1995